Q. Jl Engng Geol 1978 Vol 11 pp 219–232, 9 figs., 2 tables. Printed in Northern Ireland

Critical state parameters and peak stress envelopes for Bangkok Clays

A. S. Balasubramaniam*, **Hwang Zue-Ming**†, **Waheed Uddin**§, **A. R. Chaudhry**‖ **& Y. G. Li**‡

* Division of Geotechnical & Transportation Engineering, Asian Institute of Technology, PO Box 2754, Bangkok, Thailand.
† China Technical Consultants Inc., Taipei, Republic of China.
‡ Public Works Bureau, Taipei, Republic of China.
§ NACO, Jeddah, Saudi Arabia.
‖ Dept. of Civil Engineering, University of Basrah, Basrah, Iraq.

Summary

This paper is concerned with a detailed study of the critical state parameters and peak stress envelopes for undisturbed samples of Bangkok Clays ('Weathered Clay', 'Soft Clay' and 'Stiff Clay') taken from a site called Bangpli which is about 28 km from Bangkok. Both triaxial compression and extension tests were carried out with a wide variety of applied stress paths in a manner similar to that adopted by Parry (1960). For all types of tests the end points are presented in (q, p), $(w, \log p)$ and $(w, \log q)$ plots; q is the deviator stress, p is the mean normal effective stress and w is the water content. The Mohr Coulomb strength parameters are also evaluated for each series of tests. The results are discussed in relation to the critical state concept of Roscoe *et al.* (1958) and the water content-strength relationships of Henkel (1959).

Introduction

The work presented in this paper is an extension of that carried out by James & Balasubramaniam (1971). These authors presented data from specimens of kaolin prepared from a slurry and tested to failure from several isotropic stress states under a wide variety of imposed stress paths in a conventional axi-symmetric triaxial apparatus. Also, all the tests starting from an isotropic consolidation state (p_0) are classified into four types depending on the increments of mean normal stress and the deviator stress. The results of three types of tests at all isotropic stress levels are correlated in the 3-D space (Δe_f, p_f/p_o, q_f/p_0) in which they lie on a unique curve. Δe_f is the change in voids ratio from the pre-shear consolidation pressure to the failure state. p_f and q_f correspond to values of p and q at failure. This curve coincides with the conventional critical state line for $p_f/p_o \geq 1$ and lies on a Hvorslev type surface for $p_f/p_o < 1$.

The present paper explores the application of some of the concepts stated above for the strength behaviour of undisturbed samples of Bangkok Clays. As a first step conventional tests are carried out which included compression and extension tests (see Parry 1960). In the compression tests on 'Soft Clay' several stress paths are imposed and they include (i) undrained stress path (ii) constant p stress path and (iii) fully drained stress path.

Stress parameters used in triaxial tests

The stress parameters used in the analysis of the triaxial test results are

$$p = (\sigma'_1 + 2\sigma'_3)/3$$

and

$$q = (\sigma'_1 - \sigma'_3), \quad \text{since} \quad \sigma'_2 = \sigma'_3$$

σ'_1, σ'_2 and σ'_3 are the principal effective compressive stresses; e is the voids ratio.

General descriptions of Bangkok subsoils

The soil samples for the testing program were taken from a site called Bangpli (Nong Ngoo Hao) which is situated 28 km southeast of Bangkok. The subsoils under investigation can be divided into three main layers (see also Muktabhant 1967, and Moh *et al.* 1969):

1) 'Weathered Clay' which was formed from Soft Clay by various processes of weathering. It is an apparently overconsolidated hard crust about 4.5 m thick overlying Soft Clay.
2) Soft Clay extending to a depth of about 10 m below the weathered crust. This clay is highly compressible and is lightly overconsolidated.
3) 'Stiff Clay,' often fissured, light grey and brown in colour and extending to a depth of approximately 10 m below the Soft Clay layer. It overlies alternate layers of sand and sandy clay.

The general properties of the clays are summarized in Table 1.

TABLE 1. *General properties of Weathered, Soft and Stiff Clay*

Properties	Weathered Clay	Soft Clay	Stiff Clay
Natural water content, %	133±5	122–130	20–24
Natural voids ratio	3.86±0.15	3.11–3.64	1.10–1.30
Grain size distribution:			
Sand, %	7.5	4.0	23
Silt, %	23.5	31.7	43
Clay, %	69	64.3	34
Specific gravity	2.73	2.75±0.1	2.74
Liquid limit, %	123±2	118.5±1	46±2
Plastic limit, %	41±2	43.1±0.3	19±2
Dry unit weight, t/m^3	0.58±0.03	0.65	1.55–1.65
Consistency	Soft	Soft	Stiff
Colour	Dark grey	Greenish grey	Greenish grey
degree of saturation, %	95±2	97.8–100	94.3–100

Testing program and procedures

In this paper the results of nine series of compression tests and eleven series of extension tests are presented and discussed. They can be broadly divided into compression and extension tests performed on each of the three clay types, Weathered Clay, Soft Clay and Stiff Clay. Test samples were trimmed to a size of 36 mm diameter and 72 mm height. The procedure for taking undisturbed samples and the description for testing methods has already been presented in Balasubramaniam *et al.* (1976). In all the test series, the samples were first isotropically consolidated against an elevated back pressure. A back pressure of 414 kN/m^2 was found sufficient to dissolve all air and ensure complete saturation. Table 2 summaries the details of the testing program and the strength parameters evaluated from the tests.

Results for Weathered Clay

The maximum past consolidation pressure of Weathered Clay is about 69 kN/m^2. Compression and extension tests were therefore carried out on this clay at consolidation pressures both less than and higher than the maximum past pressure.

Compression tests

All compression tests on Weathered Clay were of the loading type wherein the lateral stress was held constant while the axial stress was increased. Series CIU-I represents undrained tests on specimens consolidated to pre-shear consolidation pressure less than the maximum past pressure. The effective stress paths of these specimens have already been presented by Balasubramaniam *et al.* (1976). The strength parameters c' and ϕ' obtained from these tests were found to be 17.3 kN/m^2 and 1.5° respectively. It is surprising to note that whereas the cohesion with respect to the effective stress is rather high, the corresponding angle of internal friction is very small. The drained compression tests carried out in Series CID-III on specimens consolidated to pre-shear consolidation pressures less than the maximum past pressure, indicated c' and ϕ' values of 9.4 kN/m^2 and 15.6° respectively. The reason for the large differences in c' and ϕ' values between undrained and drained tests will become apparent once the results of the samples consolidated to higher pre-shear consolidation pressures have been presented.

Series CIU-II represents undrained tests on specimens consolidated to pre-shear consolidation pressures higher than the maximum past pressure. The effective stress paths of these specimens have also been presented in Balasubramaniam *et al.* (1976). For these specimens c' was found to be zero and the corresponding ϕ' was 22.2°. Drained compression tests (Series CID-IV) carried out on specimens consolidated to the same pre-shear consolidation pressures also indicated virtually zero cohesion and an angle of internal friction of 23.5°. Thus the drained and undrained strength parameters on the normally consolidated specimens of Weathered Clay are virtually the same.

The results of all the four series of compression tests are presented in Figs. 1a to c in (q, p), (w, log p) and (w, log q) plots. In Fig. 1a the end points of the specimens for Series CIU-II and CID-IV, in (q, p) plot are found to lie on straight lines which pass through the origin. These straight lines correspond to the projection of the critical state line for Weathered Clay in (q, p) plot. It should be recalled that the specimens whose end points lie on the critical state line are all consolidated to pre-shear consolidation pressures higher than the maximum past pressure. However, the end points of the specimens (Series CIU-I) sheared under undrained conditions from low pre-shear consolidation pressures are found to lie on an envelope which is of very low slope in the (q, p) plot. It thus

TABLE 2. *Details of Test Series and Strength Parameters*

Test series designation	Type of clay	Type of test	Pre-shear consolidation pressure, $p_o(kN/m^2)$	Strength parameters	
				$c', kN/m^2$	ϕ'^o
CIU-I	Weathered Clay	Undrained compression loading, $p_o < p_{max}$	13.8, 20.7, 34.5, 41.4	17.3	1.5
CIU-II	Weathered Clay	Undrained compression loading, $p_o > p_{max}$	103.5, 207.0, 276, 414	0	22.2
CID-III	Weathered Clay	Drained compression loading, $p_o < p_{max}$	13.8, 27.6, 41.4	9.4	15.6
CID-IV	Weathered Clay	Drained compression loading, $p_o > p_{max}$	103.5, 207, 276	0	23.5
CIUE-V	Weathered Clay	Undrained extension unloading, $p_o < p_{max}$	10.4, 20.7, 27.6, 34.5, 41.4, 48.3	—	—
CIUE-VI	Weathered Clay	Undrained extension loading, $p_o < p_{max}$	10.4, 20.7, 27.6, 41.4, 48.3	—	—
CIDE-VII	Weathered Clay	Drained extension unloading, $p_o < p_{max}$	20.7, 27.6, 34.5, 41.4, 69	—	—
CIUE-VIII	Weathered Clay	Undrained extension unloading, $p_o > p_{max}$	103.5, 172.6, 207, 276, 345.2, 414	0	29
CIUE-IX	Soft Clay	Undrained compression loading, $p_o > p_{max}$	138, 207, 276, 345, 414	0	26
CID-X	Soft Clay	Drained compression loading, $p_o > p_{max}$	138, 207, 276, 345, 414	0	23.5
CIDP-XI	Soft Clay	Drained compression, constant p, $p_o > p_{max}$	138, 207, 276, 414	0	23.7
CIUE-XII	Soft Clay	Undrained extension loading, $p_o > p_{max}$	138, 207, 276, 345, 414	46.3	19.6
CIUE-XIII	Soft Clay	Undrained extension unloading, $p_o > p_{max}$	138, 207, 276, 345, 414	58.7	21.1
CIDE-XIV	Soft Clay	Drained extension unloading, $p_o > p_{max}$	138, 207, 276, 345, 414	31.8	23.5
CIDE-XV	Soft Clay	Drained extension loading, $p_o > p_{max}$	138, 207, 276	0	26.2
CIU-XVI	Stiff Clay	Undrained compression loading	17, 35, 70, 140, 207, 276, 345, 414, 483, 552, 620	38	24
CID-XVII	Stiff Clay	Drained compression loading	35, 105, 414, 552	30	26
CIUE-XVIII	Stiff Clay	Undrained extension unloading	138, 207, 276, 345, 414, 483, 516, 552, 621	54	25
CIUE-XIX	Stiff Clay	Undrained extension loading	34.5, 103.4, 138, 207, 276	54	18
CIDE-XX	Stiff Clay	Drained extension unloading	138, 207, 276, 348, 414, 552	11	16.6

appears that the peak stress envelope for specimens sheared under low pre-shear consolidation pressure deviates from the critical state and lies on a Hvorslev type surface (see James & Balasubramaniam 1971). It can aslo be seen from Fig. 1a that the end point for the specimen (Series CID-III) which was sheared under drained condition from the lowest pre-shear consolidation pressure (13.8 kN/m^2) lies on the same envelope as those for the specimens sheared under undrained conditions from low pre-shear consolidation pressures (Series CIU-I). However, the specimens with pre-shear consolidation pressures of 27.6 and 41.4 kN/m^2 (from Series CID-III) when sheared under drained conditions had their end points lying on the critical state line, since the mean normal stress at failure for these specimens is higher than the value that would correspond to a specimen sheared to failure under undrained conditions from pre-shear consolidation pressure equal to that of the maximum past pressure.

In Figs. 1b and c, the isotropic consolidation line for Weathered Clay is shown by dotted lines. It can be seen that the isotropic consolidation line in (w, log p) plot is curved for pressures less than the maximum past pressure and is virtually straight for mean normal stresses higher than the maximum past pressure. The isotropic consolidation curves for Weathered Clay presented in Figs. 1b and c are very similar to the corresponding characteristic curve that is normally obtained under one-dimensional consolidation in the oedometer. The slope of the isotropic consolidation line for pressures higher than the maximum past pressure is about 0.51. The end points of the specimens from all series of tests are presented in Figs. 1b and c and are found to lie on the full line drawn through these

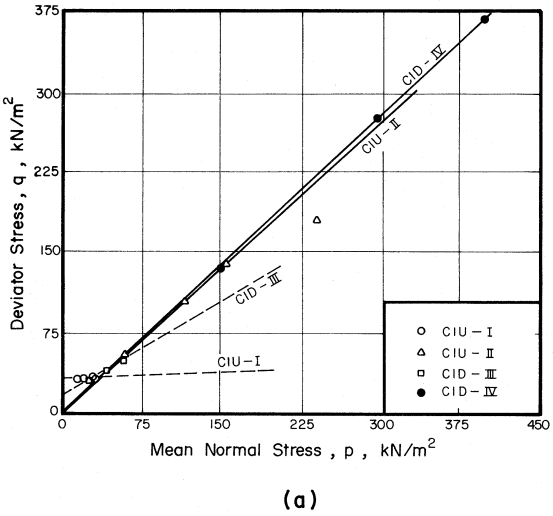

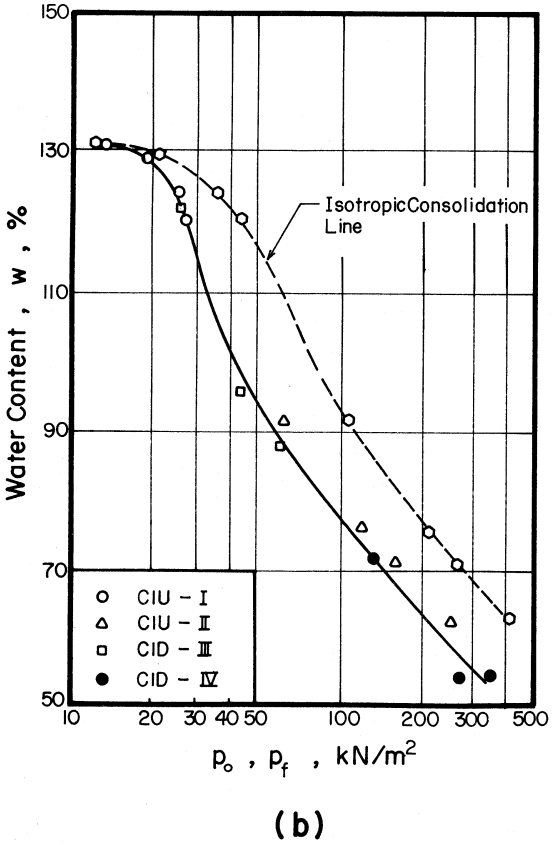

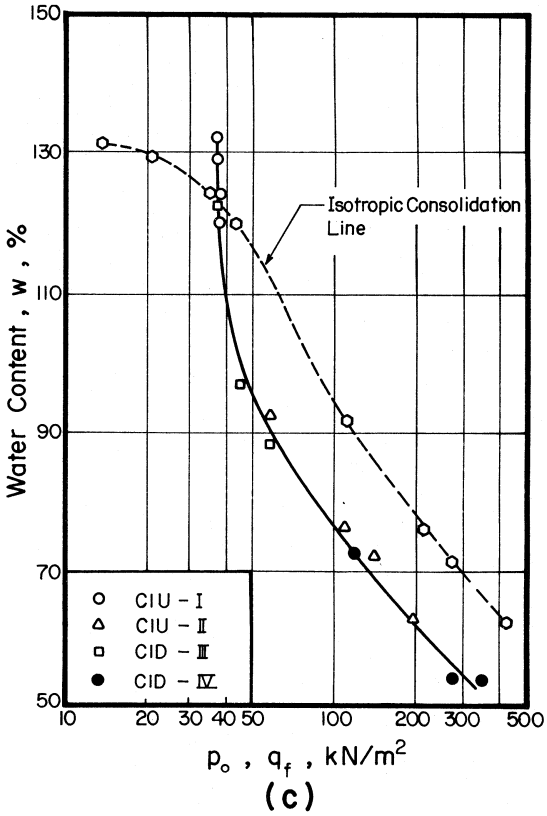

FIG. 1. Peak stress points of specimens of Weathered Clay in compression tests. (a) (q, p) plot, (b) (w, log p) plot and (c) (w, log q) plot.

points. It is interesting to note that the end points of specimens (from Series CIU-III and CID-IV) which were sheared from higher pre-shear consolidation pressures, lie close to lines which are parallel to the isotropic consolidation line in (w, log p) plot. Thus the end points of these specimens lie on the critical state line whose (q, p) projection has already been presented in Fig. 1a. However, the end points of the specimens which were sheared from pre-shear consolidation pressures less than the maximum past pressure were found to lie on an extension of the critical state line which have curved projections in (w, log p) and (w, log q) plots. These observations will be discussed further after the presentation of the extension test data.

Extension tests

Four series of extension tests were carried out on Weathered Clay. In three of these four series specimens were sheared from pre-shear consolidation pressures less than the maximum past pressure, while for

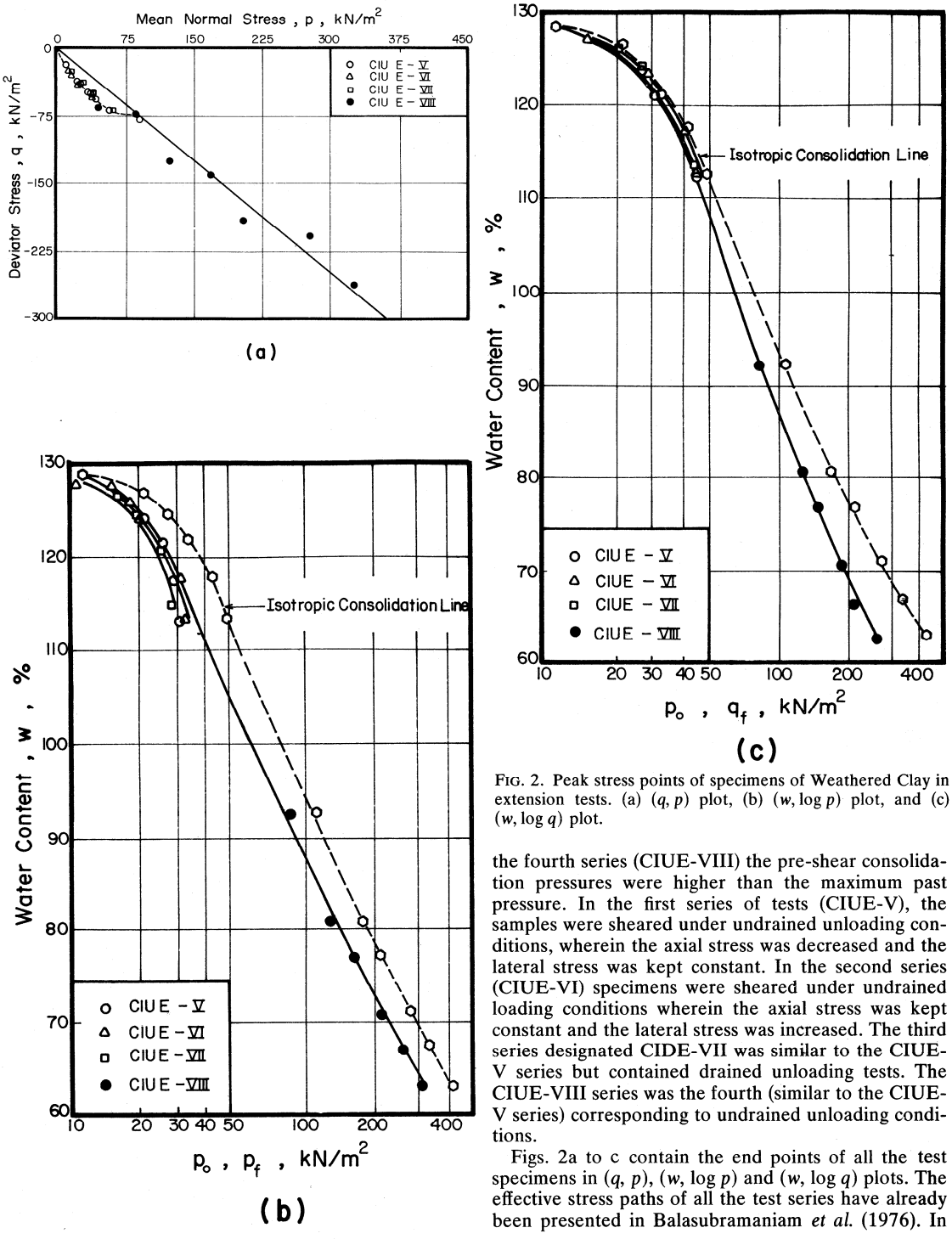

FIG. 2. Peak stress points of specimens of Weathered Clay in extension tests. (a) (q, p) plot, (b) $(w, \log p)$ plot, and (c) $(w, \log q)$ plot.

the fourth series (CIUE-VIII) the pre-shear consolidation pressures were higher than the maximum past pressure. In the first series of tests (CIUE-V), the samples were sheared under undrained unloading conditions, wherein the axial stress was decreased and the lateral stress was kept constant. In the second series (CIUE-VI) specimens were sheared under undrained loading conditions wherein the axial stress was kept constant and the lateral stress was increased. The third series designated CIDE-VII was similar to the CIUE-V series but contained drained unloading tests. The CIUE-VIII series was the fourth (similar to the CIUE-V series) corresponding to undrained unloading conditions.

Figs. 2a to c contain the end points of all the test specimens in (q, p), $(w, \log p)$ and $(w, \log q)$ plots. The effective stress paths of all the test series have already been presented in Balasubramaniam *et al.* (1976). In

Fig. 2a, the failure points of all the specimens sheared from pre-shear consolidation pressures less than the maximum past pressure (Series CIUE-V, CIUE-VI and CIDE-VII) are found to lie on a unique curved envelope shown by dotted lines. It is interesting to note that this curved envelope has a very shallow slope in the range of mean normal stresses close to the maximum past pressure. A similar observation was also noted in the earlier section for compression tests under undrained conditions on samples sheared from pre-shear consolidation pressures less than the maximum past pressure. It is thus possible that a curved failure envelope could exist even for compression conditions at very low values of mean normal stress. The results presented here for both compression and extension tests on Weathered Clay at low values of mean normal stress are in agreement with the observations made by James & Balasubramaniam (1971) on the peak stress conditions of specimens of kaolin sheared under a wide variety of applied stress paths from pressures less than the maximum past pressure.

For the specimens in Series CIUE-VIII, which were sheared from higher pre-shear consolidation pressures, the end points in Fig. 2a are found to lie on a straight line. The slope of this critical state line is 0.82 and the corresponding value of the angle of internal friction is 29°.

In Figs. 2b and c, the isotropic consolidation line is again drawn as a chain dotted line. The end points of all the test specimens are plotted in these figures. Even for the extension tests, the specimens sheared from pre-shear consolidation pressures less than the maximum past pressure have curved failure envelopes, while those sheared from higher pre-shear consolidation pressures are found to have linear projections in (w, $\log p$) and (w, $\log q$) plots which are virtually

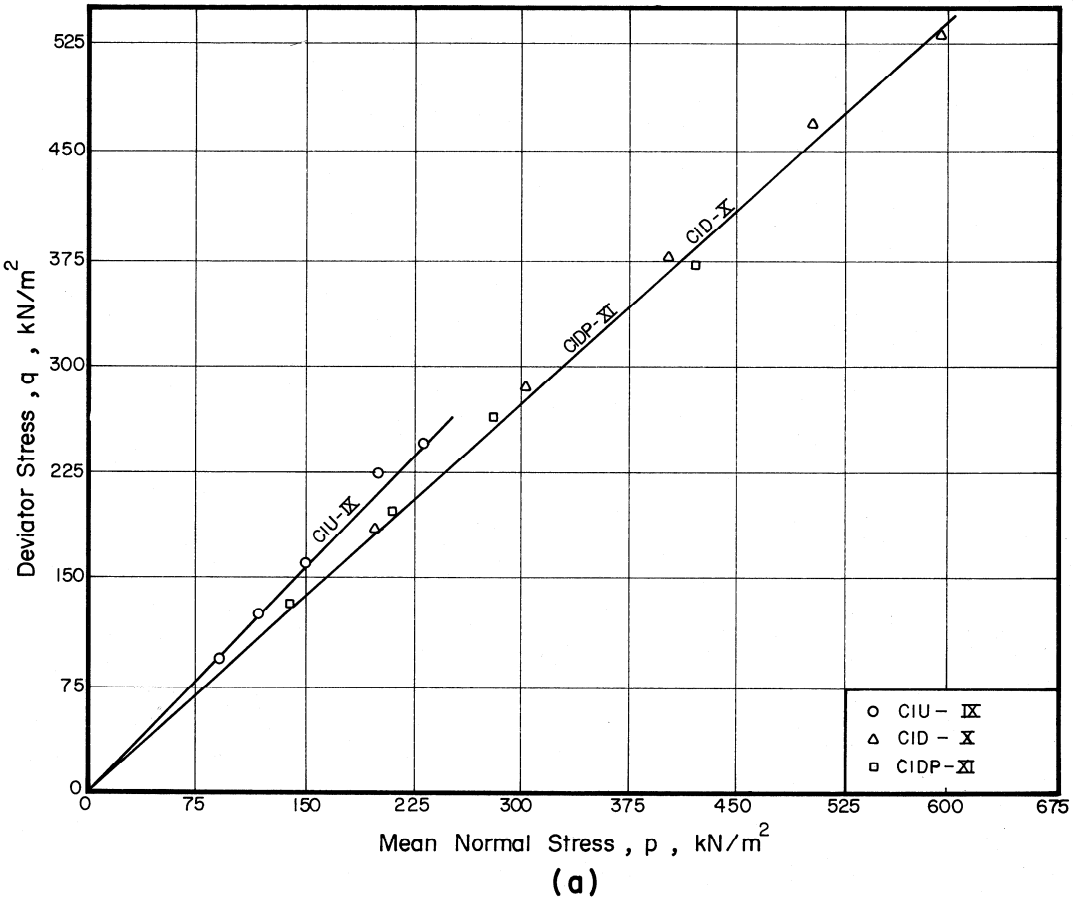

FIG. 3. Peak stress points of specimens of Soft Clay in compression tests. (a) (q,p) plot, (b) (w, $\log p$) plot and (c) (w, $\log q$) plot.

parallel to the isotropic consolidation line. It thus seems that the critical state line is straight and parallel to the isotropic consolidation line for pre-shear consolidation pressure higher than the maximum past pressure. However, for pressures less than the maximum past pressure the critical state line tends to curve and coincides with the peak strength envelope. Similar observations were also noted by Henkel (1959) and James & Balasubramaniam (1971).

Results for Soft Clay

All the compression and extension tests carried out on Soft Clay were on specimens consolidated to pre-shear consolidation pressures higher than the maximum past pressure. The effective stress paths of these specimens have already been published in Balasubramaniam *et al.* (1976).

Compression tests

Three types of compression tests were carried out and these included (i) undrained test (CIU-IX Series), (ii) fully drained tests (CID-X Series), and (iii) contant mean normal stress tests (CIDP-XI Series). All compression tests on Soft Clay were of the loading type wherein the lateral stress was held constant and axial stress increased.

Figs. 3a to c illustrate the end points of all the specimens in (q, p), $(w, \log p)$ and $(w, \log q)$ plots. The end points or the failure points are found to lie on straight lines in the (q, p) plot. The slope of the critical state line for undrained tests is 1.05 $(=M)$. the corresponding value of the angle of internal friction is 26°. The slope of the critical state line for fully drained tests was found to be nearly the same as that for constant p tests and was 0.93. The corresponding value of the angle of internal friction ϕ' was 23.7°. It is thus to be emphasised that the slope of the critical state line in (q, p) plot from undrained tests is considerably different from the slopes obtained for drained tests and constant p tests. A similar deviation was also noted by James & Balasubramaniam (1971), who argued that the critical state line is curved in $(w_f, \log p_f)$ and $(w_f, \log q_f)$plots for values of $p_f/p_o < 1$, but is straight for $p_f/p_o \geq 1$. The $(w_f, \log p_f)$ and $(w_f, \log q_f)$ relationships for all the three types of compression

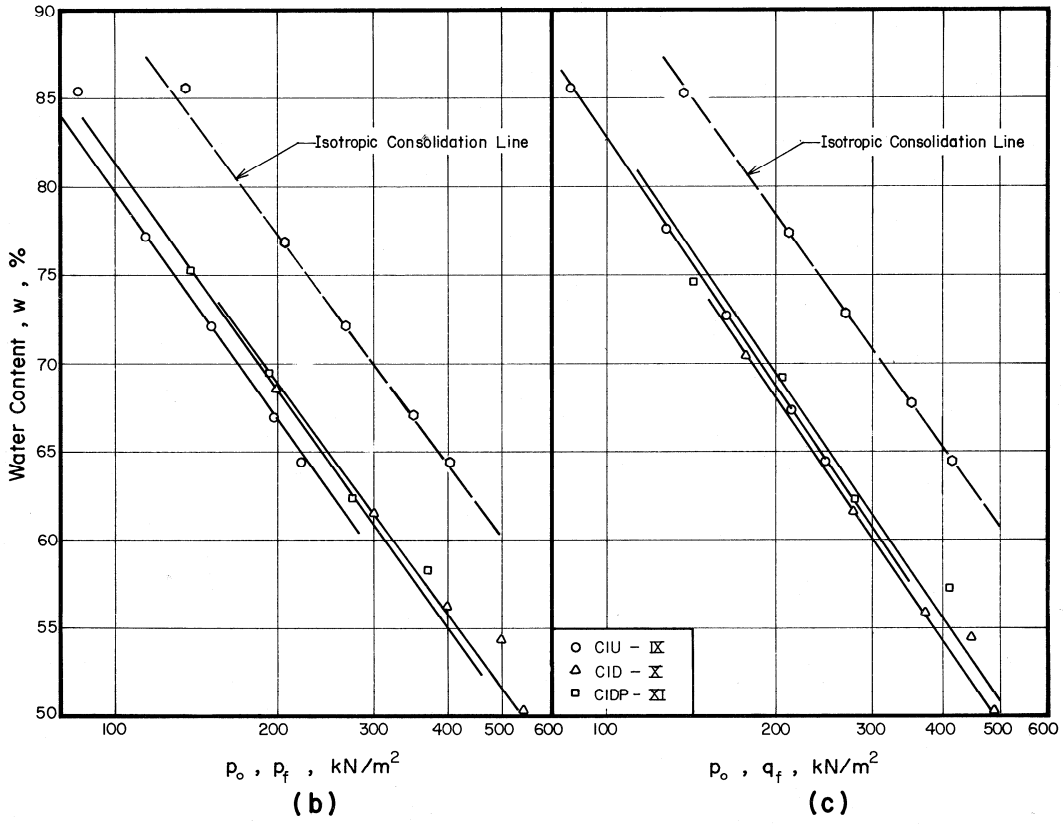

tests are presented in Figs. 3b and c and are found to be straight lines parallel to the isotropic consolidation line. Here again the end points of the undrained tests are found to lie on a line considerably displaced from the lines corresponding to fully drained and constant p tests especially in the (w_f, log p_f) plot. The slope of the isotropic consolidation line and the critical state line in (w, log p) plot is found to be 0.51.

Extension tests

Four series of extension tests were carried out on Soft Clay. Two of them were undrained tests with loading (CIUE-XII) and unloading (CIUE-XIII) conditions respectively. The other two series were drained tests (CIDE-XIV being the unloading and CIDE-XV being loading).

The end points for the specimens are presented in Figs. 4a to c. In Fig. 4a, the end points of the specimens are found to lie on straight lines in the (q, p) plot. Apparently, for all except the drained loading

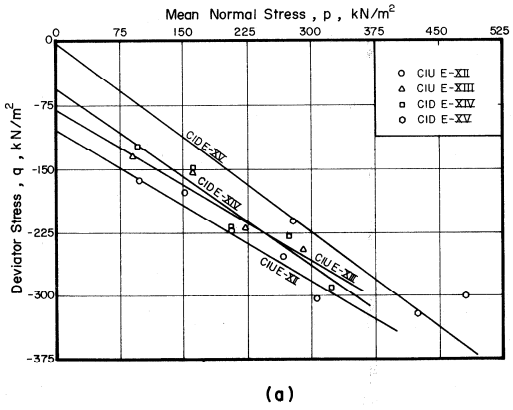

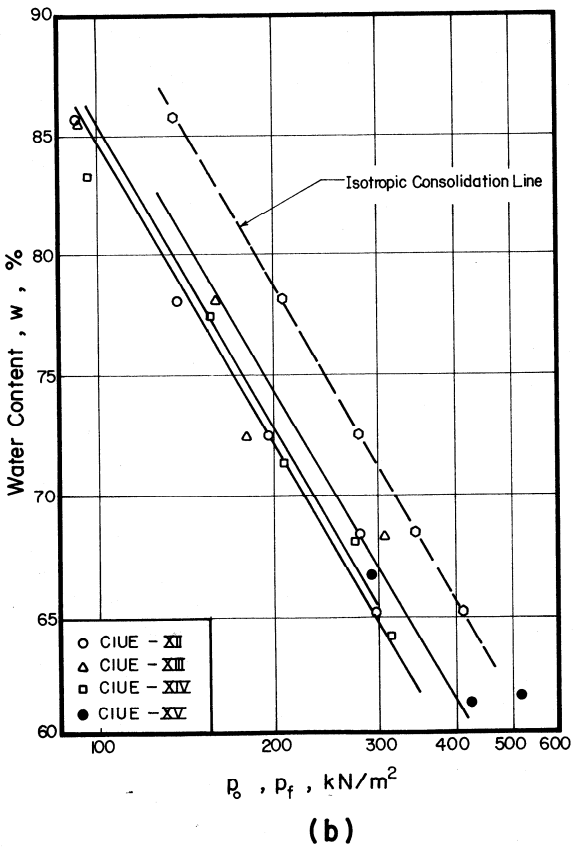

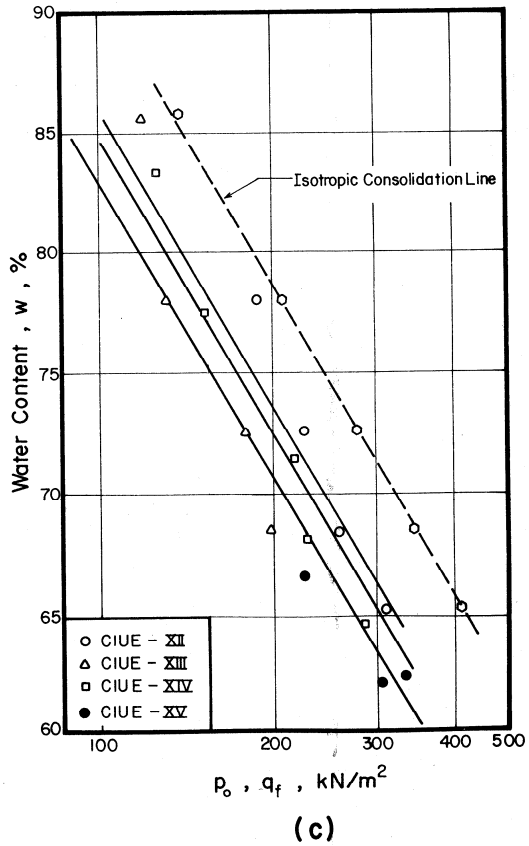

FIG. 4. Peak stress points of specimens of Soft Clay in extension tests. (a) (q, p) plot, (b) (w, log p) plot and (c) (w, log q) plot.

tests, the straight lines do not pass through the origin. The reason for this finite intercept of the failure envelope on the (q, p) plot is not clear. The Mohr's circles corresponding to failure of these specimens show c' and ϕ' values of 46.3 kN/m^2 and 19.6° under undrained loading conditions. The corresponding values under undrained unloading conditions are $c' =$ 58.7 kN/m^2 and $\phi' = 21.1°$. Thus the strength parameters under unloading conditions are slightly higher than the corresponding values under loading conditions. The drained unloading tests gave a lower c' of 31.8 kN/m^2, but showed a ϕ' of 23.5° which is higher than the values obtained from both types of drained tests. The drained loading tests gave virtually no cohesion, but the angle of internal friction was highest and was 26.2°. In Figs. 4b and c, the end points of the specimens are shown with respect to the logarithms of p and q. In both plots the end points are found to lie on straight lines which are nearly parallel to the isotropic consolidation line for Soft Clay.

Results for Stiff Clay

The natural water content of Stiff Clay (20 to 24 per cent) is considerably lower than the corresponding values for Weathered and Soft Clays (133 ± 5 per cent and 112 to 130 per cent respectively). The other index properties of Stiff Clay are also lower than those of Weathered and Soft Clay. It also contains a higher proportion of sand and silt. The conventional voids ratio-pressure relationship obtained for Stiff Clays is found to be often flat and it is not possible to obtain maximum past pressure for this clay as there is no sharp distinction on the ($e - \log p$) curves between low pressures and high pressures. The *in situ* overburden pressure for this clay is about 150 kN/m^2.

Compression tests

Only two series of compression tests were carried out on Stiff Clay and they corresponded to undrained loading conditions (CIU-XVI Series) and drained loading conditions (CID-XVII Series). The first of this series contained about eleven tests while there were only five in the second series.

The effective stress paths and the strength envelopes obtained under compression conditions are presented in Figs. 5a and b. The peak points are found to lie on straight lines in (q, p) plot for both series of tests. The strength parameters obtained from the undrained tests are $c' = 38$ kN/m^2 and $\phi' = 24°$, the corresponding values for the drained tests being $c' = 30$ kN/m^2 and $\phi' = 26°$.

Fig. 6 illustrates the (w, $\log p$) and (w, $\log q$) relationships of the peak points for both series of tests. The isotropic consolidation curve for Stiff Clay is also shown by chain dotted lines. The water content–peak stress envelopes are found to lie to the right of the isotropic consolidation curves. Also, the characteristic of the peak stress envelope for drained tests is further displaced to the right from the corresponding envelopes for undrained tests. For both types of tests the (w_f, $\log p_f$) and (w_f, $\log q_f$) relationships are curved, but are not similar in shape to the corresponding isotropic consolidation curve.

Extension tests

Altogether three series of extension tests were carried out on Stiff Clay. These corresponded to undrained unloading (CIUE-XVIII Series), undrained loading (CIUE-XIX Series) and drained unloading (CIDE-XX Series) conditions. The effective stress paths and the strength envelopes of these specimens are presented in Figs. 7a to c. The undrained test specimens virtually had the same cohesion of $c' =$ 54 kN/m^2. However, the angle of internal friction for the unloading conditions is 25°, while that for loading conditions is only 18°. Drained extension unloading specimens were found to have the least strength parameters of $c' = 11$ kN/m^2 and ϕ' of 16.6°.

The (w_f, $\log p_f$) and (w_f, $\log q_f$) relationships for all the test series are presented in Figs. 8a and b. In these figures, the isotropic consolidation line is also represented by chain dotted lines. For specimens sheared at higher pre-shear consolidation pressures, the water content–peak stress envelopes are found to cross the isotropic consolidation line from the right (at low pressures) to the left at higher pressures. The failure envelopes are found to be curved, but are not parallel to the isotropic consolidation curve. The (w_f, $\log p_f$) relationship at pressures less than 300 kN/m^2 can be approximated as a single curve. For pressures higher than 300 kN/m^2, the CIUE-XVIII Series and the CIDE-XX Series are found to give different characteristics. For all series of tests, the (w_f, $\log q_f$) relationships are different for the whole range of pressures.

Comparison of the behaviour of Weathered Clay, Soft Clay and Stiff Clay

A comparison will now be made of the three types of clays with respect to strength parameters and water content strength relationships. For Weathered Clay tested under pre-shear consolidation pressures less than the maximum past pressure, the cohesion is found to be comparatively high and the angle of internal friction is small. Under extension conditions, the strength envelopes at low pressures are curved indicating that both c' and ϕ' are dependent on the pre-shear consolidation pressure and the type of applied stress path taken to failure.

However, when Weathered Clay was consolidated to pressures higher than the apparent maximum past

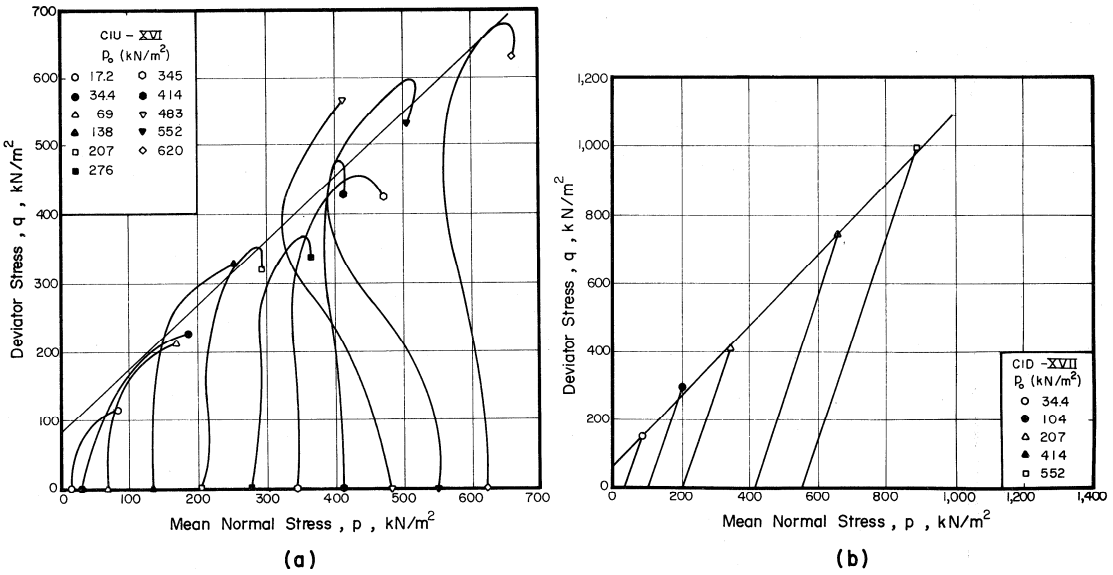

FIG. 5. Stress paths and peak stress envelopes in (q,p) plot for Stiff Clay during compression. (a) undrained loading tests, (b) drained loading tests.

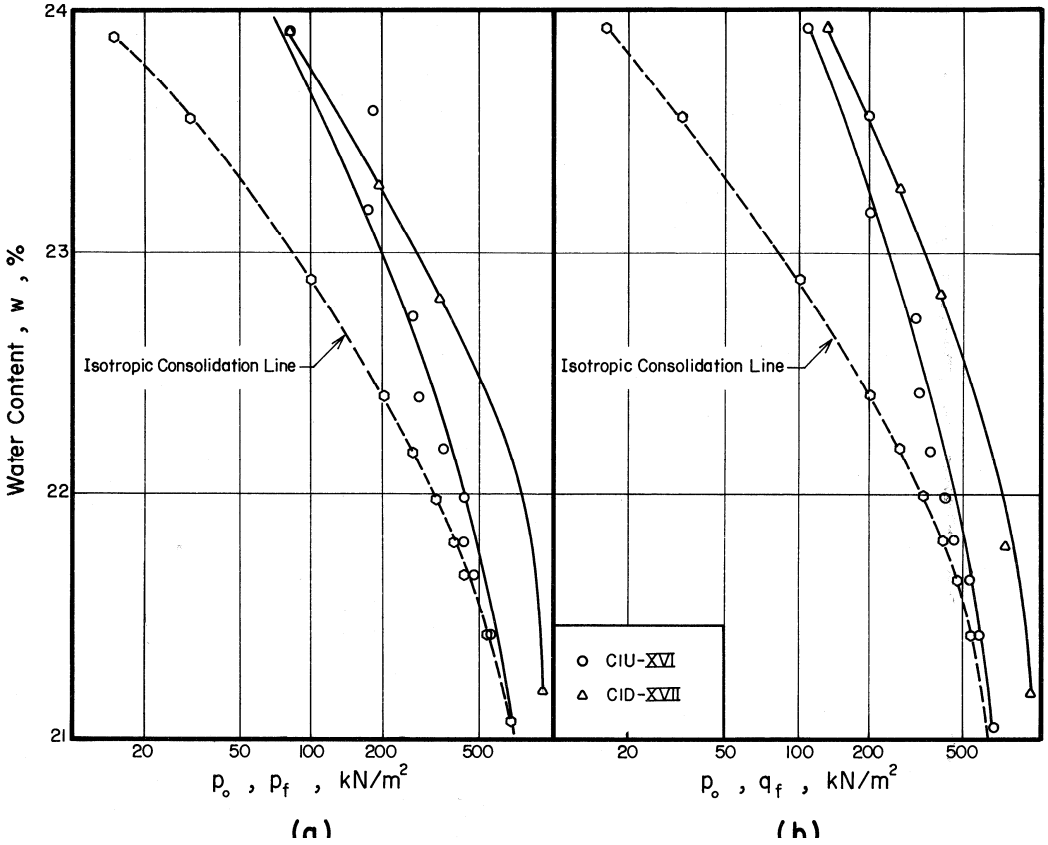

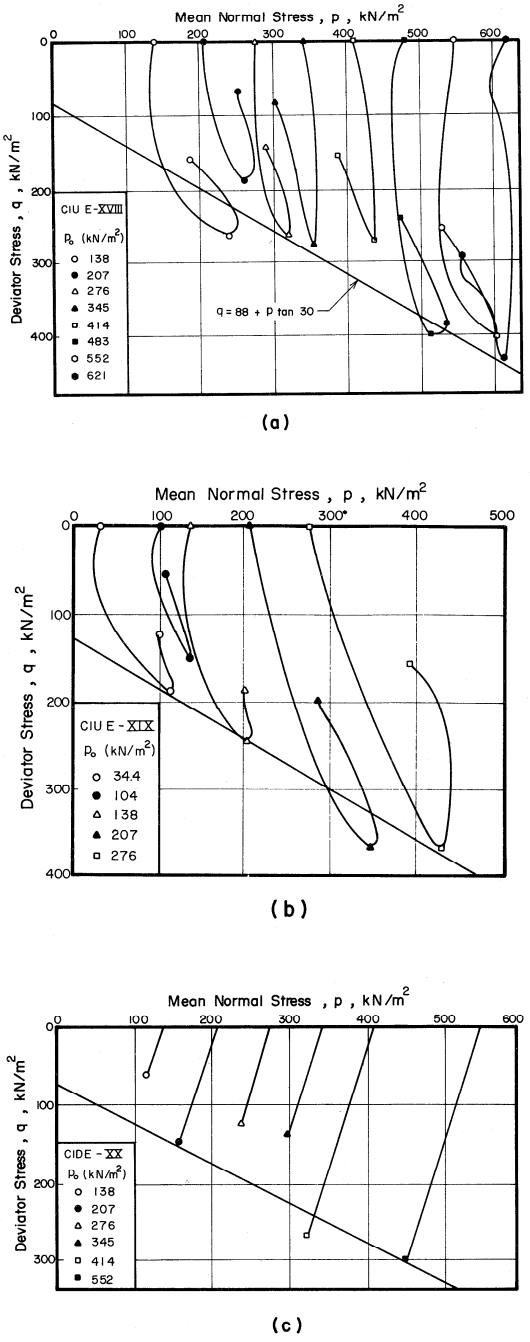

FIG. 7. Stress paths and peak stress envelopes in (q,p) plot for Stiff Clay during extension. (a) undrained unloading tests (b) undrained loading tests and (c) drained unloading tests.

pressure (caused by weathering etc.), the Weathered Clay was found to behave very nearly the same as Soft Clay. When the pre-shear consolidation pressure is higher than the maximum past pressure during compression conditions both Weathered Clay and Soft Clay are found to have virtually zero cohesion and the angle of internal friction is also of the same order of magnitude, though the value obtained from undrained tests on Soft Clay is slightly higher. Also, the angle of internal friction obtained for Weathered Clay under undrained unloading conditions in extension tests is considerably higher than the values obtained from all other tests. Except for these differences, it seems that Weathered Clay possesses the same strength parameters as that of Soft Clay when both are sheared from pre-shear consolidation pressures higher than the maximum past pressure.

Fig. 9 corresponds to the $(w_f, \log p_f)$ and $(w_f, \log q_f)$ relationships when all the three types of clays were sheared under undrained compression loading conditions. In Fig. 9, the curves drawn as dotted lines represent the isotropic consolidation tests. It is interesting to note that the isotropic consolidation curve for Weathered Clay at pressures higher than the maximum past pressure coincides with the corresponding characteristics for Soft Clay. This perhaps is also an indication that both clays have the same geological origin and mineralogical composition. It should be recalled that the natural water content and other index properties for these clays are also nearly the same. The Stiff Clay has an isotropic consolidation curve completely different from those of Weathered Clay and Soft Clay. For Weathered Clay, in all tests with mean normal stresses less than the maximum past pressure, the isotropic consolidation curve and the failure envelopes are both curved. However, for pressures higher than the maximum past pressure, the isotropic consolidation curve and the water content–strength relationships are virtually parallel and straight. These observations are in general agreement with the critical state concept of Roscoe *et al.* (1958) and the water content–strength relationships of Henkel (1959). The results obtained from samples sheared under other types of stress conditions (namely drained compression loading, undrained extension loading, undrained extension unloading and drained extension unloading respectively) also confirm the same findings.

Conclusions

A comprehensive series of compression and extension tests were carried out on Weathered, Soft and Stiff Bangkok Clay in the triaxial apparatus to study the peak stress conditions under various types of applied stress paths. The extension tests were carried out under unloading and loading conditions. The compression tests on Soft Clay are of three types; undrained test, constant p test and fully drained test. For all

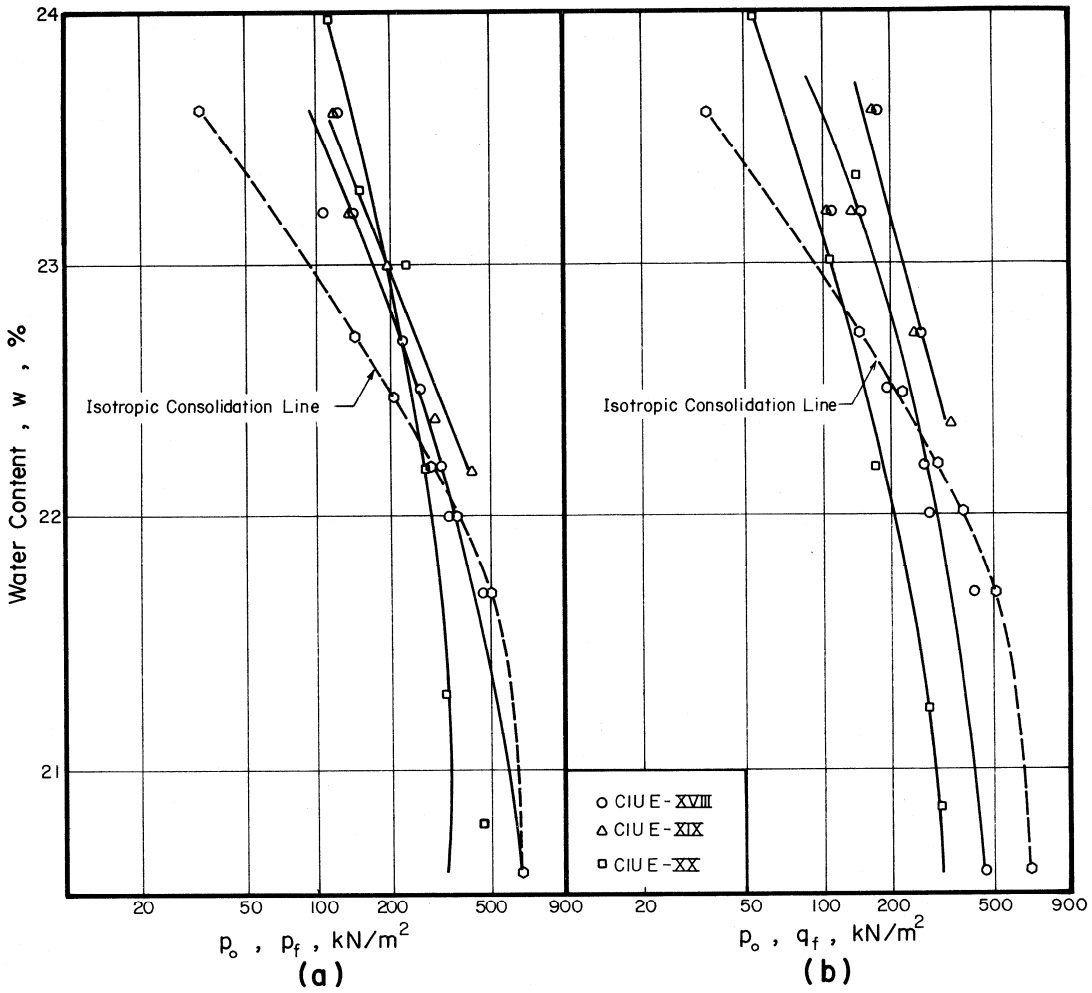

FIG. 8. Peak stress points of specimens of Stiff Clay during extension tests. (a) (w, log p) plot, (b) (w, log q) plot.

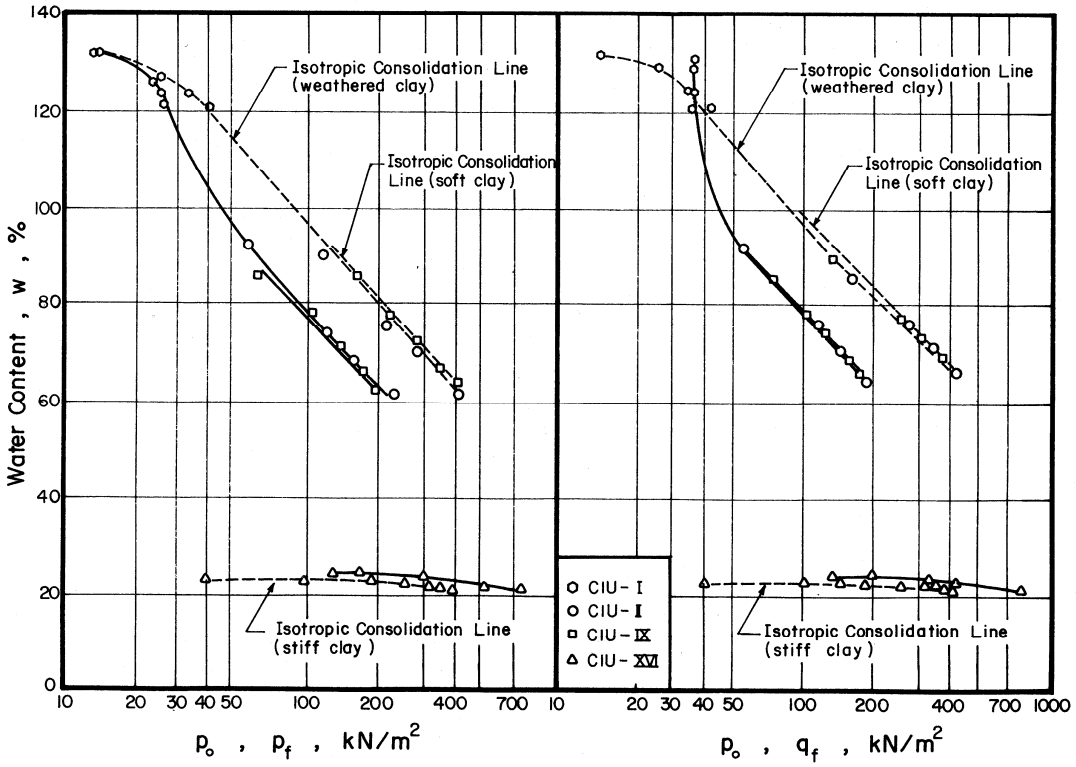

FIG. 9. Water content-peak stress relationships for all clays during undrained compression loading tests.

types of tests the end points are presented in (q, p), (w, log p) and (w, log q) plots. Also, the Mohr Coulomb strength parameters are evaluated for each series of tests. The results are in general agreement with the previous work carried out by a number of workers, (see Roscoe *et al.* 1958, Henkel 1959, Parry 1960 and James & Balasubramaniam 1971) on remoulded specimens of kaolin and other clays.

ACKNOWLEDGEMENTS. The work presented in this paper was carried out at the Asian Institute of Technology. The authors would like to express their deep gratitude to Mr Gamini Adikari, for his assistance in compiling the data. The triaxial tests on Stiff Clay were performed by Messrs Hasan Zahurul and Md. Aftabuddin Ahmed. Thanks are also due to Messrs Ruangvit Chotivitayathanin and Suvit Viranuvut for their assistance in carrying out the experimental program, and to Profs Za-Chieh Moh, Edward W. Brand, Mrs Vatinee Chern and Mrs Uraivan Singchinsuk for their continuous support and encouragement.

References

BALASUBRAMANIAM, A. S., CHAUDHRY, A. R., HWANG, Z. M., WAHEED UDDIN & LI, Y. G. 1976. State Boundary Surface for Weathered and Soft Bangkok Clay. *Aust. Geomechanics J.* **6,** 43–50.

HENKEL, D. J. 1959. The Relationships between the Strength, Pore Water Pressure and Volume Change Characteristics of Saturated Clays. *Géotechnique* **9,** 119–35.

JAMES, R. G. & BALASUBRAMANIAM, A. S. 1971. The peak Stress Envelopes and their Relation to the Critical State Line for a Saturated Clay. *Proc. 4th Asian Reg. Confr. Soil Mech. & Found. Engng, Bangkok,* **1,** 115–20.

MOH, Z. C., NELSON, J. D. & BRAND, E. W. 1969. Strength and Deformation Behaviour of Bangkok Clay. *Proc. 7th int. Confr. Soil Mech. & Found. Engng, Mexico,* 287–95.

MUKABHANT, C. 1967. Engineering properties of Bangkok subsoils. *Chulalongkorn Univ. Rep., Bangkok.*

PARRY, R. H. G. 1960. Triaxial Compression and Extension Tests on Remoulded Saturated Clay. *Géotechnique* **10,** no. 4, 166–80.

ROSCOE, K. H., SCHOFIELD, A. N. & WROTH, C. P. 1958. On the Yielding of Soils. *Géotechnique* **8,** 22–53.

Notations

e	voids ratio
e_o	pre-shear voids ratio
Δe	change in voids ratio
M	slope of critical state line in (q, p) plot
p	mean normal stress
p_o	pre-shear consolidation pressure
$(p_o)_{max}$	maximum value of isotropic consolidation pressure
q	deviator stress
w	water content
$\sigma'_1, \sigma'_2, \sigma'_3$	principal effective compressive stress
ϕ'	angle of internal friction

Suffix f denotes failure.